processes

Article

Slow-Release Urea Fertilizer with Water Retention and Photosensitivity Properties Based on Sodium Alginate/Carboxymethyl Starch Sodium/Polydopamine

Yan Li [1], Yu Ma [1], Fan Chang [1], Haiyun Zhu [1], Chengshan Tian [2], Fengan Jia [1], Yang Ke [1] and Jiakun Dai [3,*]

[1] Shaanxi Institute of Microbiology, Xi'an 710043, China; liyanwsw@126.com (Y.L.); wefly@xab.ac.cn (Y.M.); fanchang_509@163.com (F.C.); zhuhaiyun@xab.ac.cn (H.Z.); jiafenganwsw@163.com (F.J.); keyang-bio@163.com (Y.K.)
[2] Shaanxi Zhongkewanjia Agricultural Company, Xi'an 710043, China; sxglkx@126.com
[3] Bio-Agriculture Institute of Shaanxi, Xi'an 710043, China
* Correspondence: djkxa@163.com

Abstract: Using slow-release fertilizer is one of the sustainable strategies to improve the effectiveness of fertilizers and mitigate the environmental pollution caused by excess usage of fertilizer. In this study, a slow-release urea fertilizer with water retention and photosensitivity properties was prepared by a two-step method. It was characterized by Fourier transform infrared spectroscopy, thermogravimetric analysis, scanning electron microscopy and an infrared camera. This fertilizer can prolong the release period of urea, improve water-retention capacity of soil, and carry out photothermal conversion under illumination. Comparing four release kinetics models, the Ritger–Peppas model was the best fitting model for releasing behavior in soil, and diffusion followed the Fickian mechanism. The application of fertilizer on winter wheat was carried out to intuitively evaluate the fertilizer's effects on promoting plant growth and resisting water stress. Thus, this study provides a new strategy for improving fertilizer utilization rate and maintaining soil moisture, which will be beneficial for sustainable agriculture.

Keywords: slow-release fertilizer; urea; water retention; sodium alginate; carboxymethyl starch sodium; polydopamine

Citation: Li, Y.; Ma, Y.; Chang, F.; Zhu, H.; Tian, C.; Jia, F.; Ke, Y.; Dai, J. Slow-Release Urea Fertilizer with Water Retention and Photosensitivity Properties Based on Sodium Alginate/Carboxymethyl Starch Sodium/Polydopamine. *Processes* **2024**, *12*, 842. https://doi.org/10.3390/pr12040842

Academic Editor: Olaniyi Amos Fawole

Received: 1 March 2024
Revised: 3 April 2024
Accepted: 18 April 2024
Published: 22 April 2024

1. Introduction

Light, water, and temperature are considered the most important factors during crop growth. In areas with low precipitation, soils with a high water-retention capacity can reduce the influence of drought on crops [1]. Soil temperature affects the growth of crop roots and the cycle of nutrient elements [2]. Increasing the moisture and temperature of soil can improve crop germination, promote the growth process, and thus contribute to a higher yield.

With the continuous growth of the population, a large number of chemical fertilizers, such as urea, are used to ensure the yield of grain. However, more than 50% of fertilizers are lost because of volatilization, leaching, and chemical hydrolysis [3,4]. To ensure the food supply, chemical fertilizer has been overused, which damages soil structure and causes soil hardening [5,6]. Furthermore, the rapid infiltration of chemical fertilizer makes it difficult for plants to absorb all nutrients. Nutrients accumulate and leach into groundwater, resulting in water eutrophication and serious agricultural non-point source pollution [7,8]. To improve the utilization rate of chemical fertilizers and reduce the total amount of chemical fertilizers, slow-release fertilizers (SRFs) have been gradually applied to agricultural production [9–11].

In recent years, biodegradable and environmentally friendly materials used in SRFs have attracted much attention. Sodium alginate (SA) is a natural biodegradable polymer with high gelation ability that has been used as a good material for SRFs [12]. However, after solidifying into dry particles, its water absorption is low. Carboxymethyl starch sodium (CMS) is an important derivative of starch. CMS is not only biodegradable but also has good water absorption, and is widely used in food, textiles, and medicine. However, its low mechanical strength limits its application in agriculture [13]. Dopamine (DA), as a biodegradable and non-toxic photosensitizer, has good photothermal conversion efficiency and can spontaneously adhere to the surface of materials to form a polydopamine film [14,15]. In addition, dopamine can significantly improve plant growth, chlorophyll content, and root development. It can regulate nitrogen absorption and metabolism by enhancing activities of enzymes related to nitrogen metabolism [16]. However, reported studies about dopamine in the field of agriculture are rare.

In this study, sodium alginate (SA) and carboxymethyl starch sodium (CMS) were compounded to form a composite network core to embed urea, and a polydopamine (PDA) film was formed on its surface by using the self-polymerization adsorption of dopamine. The physical and chemical properties, water retentivity and photosensitivity, release kinetics models, and winter wheat application of the SRF were investigated for the evaluation of the feasibility in sustainable agriculture.

2. Materials and Methods

2.1. Experimental Materials

Sodium alginate (viscosity: 200 ± 20 mpa·s, Mw: 198.11), carboxymethyl starch sodium, calcium chloride, urea, and dopamine hydrochloride were purchased from Aladdin Chemical Technology Co. , Ltd. (Shanghai, China); Tris-HCl (pH 8.5) and p-dimethylaminobenzaldehyde were purchased from Sinopharm Chemical Reagents Co., Ltd. (Shanghai, China); ethanol and hydrochloric acid were purchased from Nanjing Chemical Reagent Co., Ltd. (Nanjing, China); and winter wheat (Jimai 23) was supplied by the Crop Research Institute of Shandong Academy of Agricultural Sciences.

2.2. Preparation of Sodium Alginate/Carboxymethyl Starch Sodium/Polydopamine/Urea

Sodium alginate (0.6 g) was added into distilled water (20 mL) and heated (70 °C) with stirring to dissolve. Carboxymethyl starch sodium (0.5 g) was dissolved in distilled water (10 mL). Then, the solutions of sodium alginate and carboxymethyl starch sodium were mixed evenly, and added to urea (3 g). Afterward, the mixed solution was dripped into calcium chloride solution (2%) to solidify into gelatinous particles, with an autosampler at a constant speed. The gelatinous particles of sodium alginate/carboxymethyl starch sodium/urea (SCU) were collected by filtration, washed with distilled water three times, and dried at room temperature.

Then, dopamine hydrochloride (500 mg) was added to Tris-HCl (10 mM, pH 8.5). Subsequently, SCU particles were added and stirred slowly for 5 min. Dopamine in the solution polymerized spontaneously on the surface of SCU particles, thus forming sodium alginate/carboxymethyl starch sodium/polydopamine/urea (SCPU). Finally, SCPU particles were collected by filtration, washed with distilled water, and dried at room temperature.

2.3. Characterization

The structures of SA, CMS, PDA, urea, and SCPU were characterized by Fourier transform infrared (FTIR) spectroscopy (Thermo Fisher Nicolet 5700, Waltham, MA, USA), and the FTIR spectra were obtained in wavenumber range from 400 to 4000 cm^{-1} with KBr disks. Thermogravimetric analysis (TGA) was performed with a thermogravimetric analyzer (Mettler Toledo TGA 1600HT, Greifensee, Switzerland), and the heating rate was 10 °C/min from 25 °C to 900 °C under a nitrogen atmosphere. The surface morphology of sodium alginate/urea (SU), SCU and SCPU particles was characterized by scanning electron microscopy (SEM, JEOL JSM-IT500, Tokyo, Japan). Before testing, the samples were sputtered with gold.

2.4. Water Absorption of SCPU

A certain amount of SU, SCU, and SCPU particles were soaked in 100 mL distilled water until the swelling was balanced. After removing the residual water from the particle surface with absorbent paper, the water absorption (*WA*) was calculated using Equation (1) [17] as follows:

$$WA\ (\%) = (W_s - W_d)/W_d \times 100\% \tag{1}$$

where W_s is the saturated weight of sample and W_d is the dry weight of sample.

2.5. Water-Holding Capacity and Water-Retention Behavior of SCPU

Soil was dried to constant weight at room temperature and was passed through a 20-mesh sieve. Then, the soil (40 g) was mixed with SCPU (3 g or 5 g) and added into a PVC pipe (diameter of 3 cm), with the bottom sealed with gauze. Distilled water was added slowly from the top of the PVC pipe until it seeped from the bottom of the pipe. When no more water dripped from the bottom, the pipe was weighed again. The maximum water-holding (*WH*) capacity was calculated using Equation (2) [18] as follows:

$$WH\ (\%) = (W_1 - W_0)/W \times 100\% \tag{2}$$

where W is the total mass of the soil and SCPU, W_0 is the total mass of the soil, SCPU, and PVC pipes, and W_1 is the total mass of the water, soil, SCPU, and PVC pipes.

A mixture of soil (40 g) and SCPU (5 g) was placed in a glass beaker (50 mL). Distilled water was added into the beaker slowly to penetrate into the soil, and then the beaker was weighed. The beaker was placed at room temperature and weighed every two days, and the observation was carried out for 20 days. The water retention (*WR*) was calculated using Equation (3) [19] as follows:

$$WR\ (\%) = (W_t - W_0)/(W_1 - W_0) \times 100\% \tag{3}$$

where W_0 is the total mass of soil, SCPU, and beaker, W_1 is the total mass of water, soil, SCPU, and beaker, and W_t is the total mass of water, soil, SCPU, and beaker after a certain time interval.

2.6. Slow-Release Behavior of SCPU

The soil was washed with distilled water to remove the soluble matter completely and dried. Then, the soil (500 g) was mixed with SCPU (5 g) and packed into a PVC column (diameter 10 cm, height 40 cm). An appropriate amount of sand was added at the top of the soil to reduce interference. Absorbent cotton was placed at the bottom of the column to prevent clogging. At a certain time interval, 50 mL distilled water was slowly added to the soil column, and leachate was collected at the bottom of the column with a triangular bottle. The amount of urea released was analyzed using a spectrophotometer to compare the slow-release behavior of urea and SCPU particles [20].

2.7. Release Kinetics of SCPU

The zero-order model, first-order model, Higuchi model, and Ritger–Peppas model were used to simulate the release kinetics of SCPU slow-release fertilizer [21–23].

$$\text{Zero-order model: } M_t/M_\infty = k_0\, t \tag{4}$$

$$\text{First-order model: } M_t/M_\infty = 1 - e^{-k1t} \tag{5}$$

$$\text{Higuchi model: } M_t/M_\infty = k_H\, t^{1/2} \tag{6}$$

$$\text{Ritger-Peppas model: } M_t/M_\infty = k_R\, t^n \tag{7}$$

where t is the release time, and M_t and M_∞ are the urea mass at a particular release time 't' and at equilibrium, respectively. N is the diffusion exponent of the Ritger–Peppas model. k_0, k_1, k_H, and k_R are release constants in the zero-order model, first-order model, Higuchi model, and Ritger–Peppas model, respectively.

2.8. Photothermal Conversion Performance of SCPU

For measuring the photothermal conversion performance, the Petri dish (diameter 5 cm) was covered with a certain amount of SCU and SCPU microspheres, and then irradiated by the sunlight of 120 mW/cm^2 for 5 min. The temperature variation of the samples at different time intervals were monitored by an infrared camera.

2.9. Plant Growth Experiment

The soil was collected from the experimental field of Bio-Agriculture Institute of Shaanxi, Xi'an, Shaanxi province, China (34°16′ N, 108°54′ E). The properties of soil were 11.9 g·kg^{-1} (soil organic matter), 0.79 g·kg^{-1} (total N), 59.7 mg·kg^{-1} (available N), 80.7 mg kg^{-1} (Olsen-P), 249.3 mg kg^{-1} (exchangeable K), and pH 8.14.

Urea (0.2 g), 1× SCPU (containing 0.2 g urea), and 2× SCPU (containing 0.4 g urea) were mixed in soil (2000 g) with untreated soil as a control. Then, the soil was moved into flowerpots (diameter 15 cm). A total of 25 winter wheat seeds were planted in each flowerpot, and were then placed in a greenhouse (18 °C) for observation. Three replicates were conducted for each treatment. The plants were watered every 4 days (200 mL), and watering was stopped on the 16th day. The growth of winter wheat in different soil treatments under moisture and drought conditions were compared.

2.10. Statistical Analysis

The data were statistically analyzed by ANOVA with the SPSS software package (version 26.0) for Windows. Means were compared by the least significant difference (LSD) test at the 0.05 probability level.

3. Results and Discussion

3.1. FTIR Analysis

The FTIR spectra of sodium alginate, carboxymethyl starch sodium, dopamine, urea, and SCPU are shown in Figure 1. In the spectrum of sodium alginate, the characteristic absorption peak at 1028 cm^{-1} was associated with the C-O stretching vibration [24]. For carboxymethyl starch sodium, the absorption peaks at 1593 cm^{-1} and 1151 cm^{-1} were attributed to the C=O stretching vibration of carboxylic acid group (-COO) and the C-O-C bond vibration of glycoside, respectively [25,26]. In the spectrum of dopamine, the characteristic absorption peaks at 1282 cm^{-1}, 1608 cm^{-1}, and 3332 cm^{-1} were the stretching vibrations of C-O, C=C of the benzene ring, and N-H groups, respectively [27–29]. In the spectrum of urea, the absorption peaks at 1675 cm^{-1} and 3427 cm^{-1} were due to the stretching of C=O and N-H bonds, respectively [30]. Furthermore, these characteristic peaks of sodium alginate, sodium carboxymethyl starch, polydopamine, and urea were also observed in the FTIR spectrum of SCPU, which confirmed the successful preparation of SCPU.

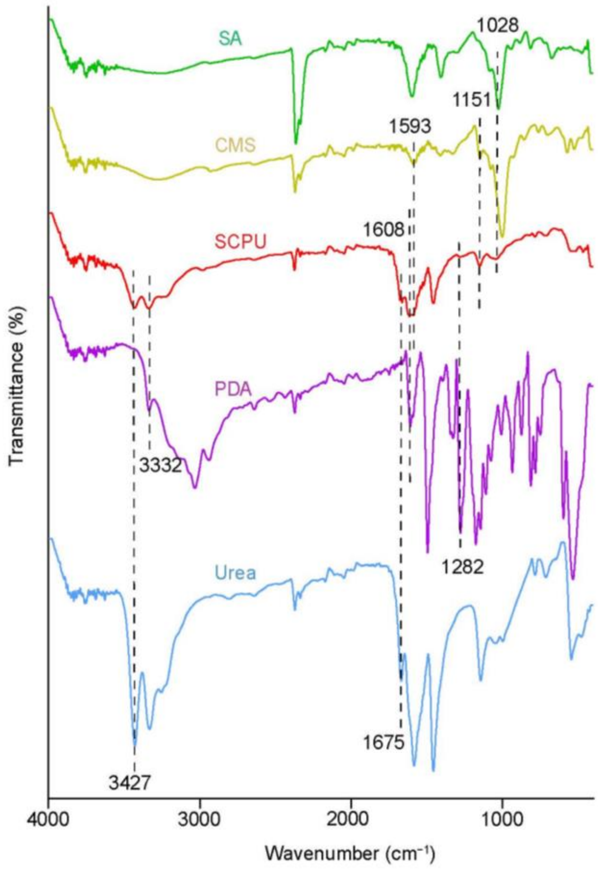

Figure 1. FTIR spectra of sodium alginate, carboxymethyl starch sodium, dopamine, urea, and SCPU.

3.2. Thermogravimetric Analysis

The thermal stability of all related materials was investigated by thermogravimetric analysis (TGA) in a nitrogen atmosphere (Figure 2A). The loss of all the materials at approximately 100 °C was related to a small amount of adsorbed water and bound water [31]. In the thermal decomposition curve of urea, decomposition started at 130 °C and ended at approximately 400 °C. At temperatures above 400 °C, the residual content was almost zero, which was consistent with relevant reports [32]. Sodium alginate was dehydrated before 200 °C. It cracked to form intermediate products at 200–260 °C. When the temperature rose from 260 °C, the intermediate products continued to be cracked and carbonized, with approximately 31% remaining at 800 °C [33]. The maximum weight loss of carboxymethyl starch sodium occurred at 225–320 °C, which was mainly related to the breaking of C-O-C bond in carboxymethyl starch sodium and the loss of carbon dioxide. When the temperature reached 800 °C, the residue was approximately 19% [34]. Although obvious thermal decomposition of dopamine can be observed at 256–430 °C, the residue can still reach 28% at 800 °C. Furthermore, when dopamine forms as a polymer, it will undergo a gradual thermal decomposition, and the residue can reach over 40% at 800 °C [35]. The thermal degradation process of SCPU was a comprehensive reflection of sodium alginate, carboxymethyl starch sodium, dopamine, and urea. SCPU showed obvious thermal decomposition at 160–320 °C, and gradually decomposed above 320 °C. The residual rate at 800 °C was 7.7%, which was between the rates of related materials.

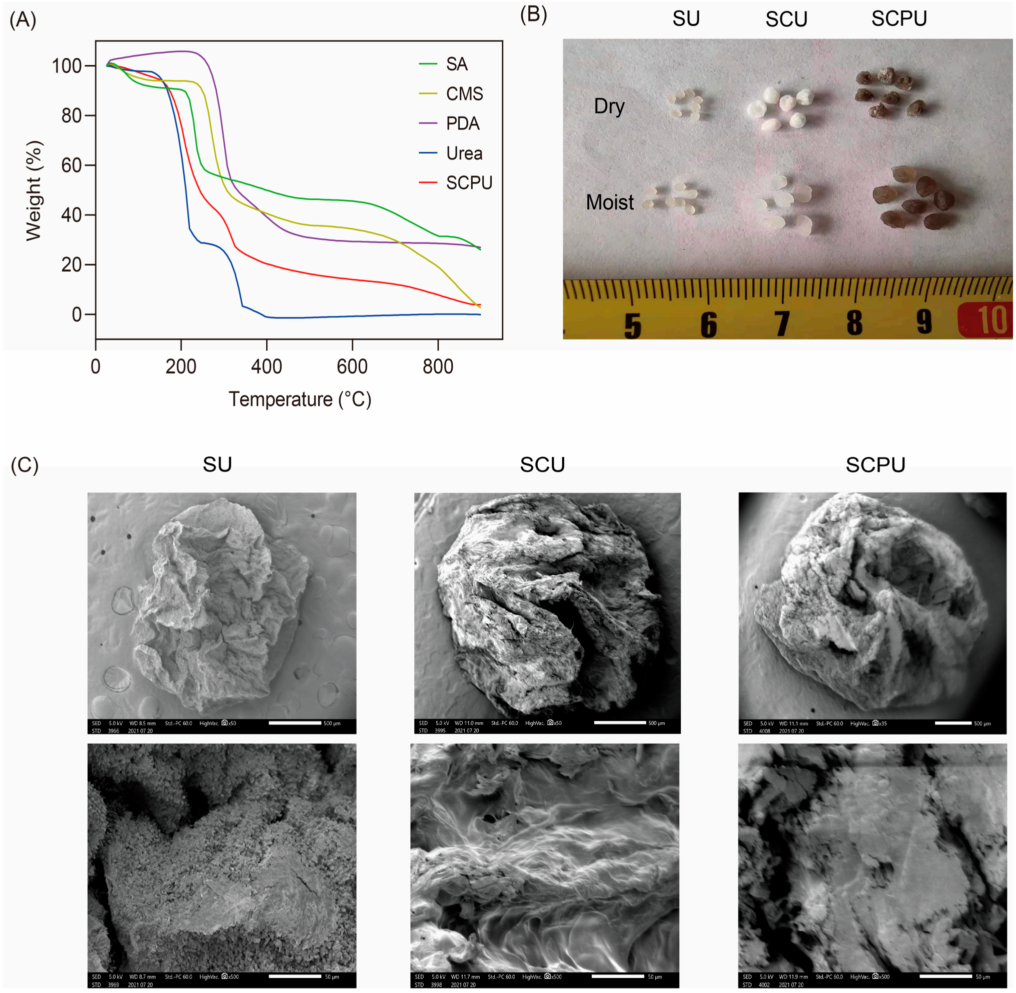

Figure 2. (**A**) TGA curves of all the materials. (**B**) Morphology of SA/urea (SU), SA/CMS/urea (SCU), and SA/CMS/PDA/urea (SCPU) before and after swelling. (**C**) Scanning electron microscope images of SU, SCU, and SCPU.

3.3. SEM Analysis

The morphology before and after swelling and the scanning electron microscope images of SA/urea (SU), SA/CMS/urea (SCU), and SA/CMS/PDA/urea (SCPU) are shown in Figure 2B and C, respectively. SA/urea was a kind of translucent particle, and its morphology had no obvious change after water absorption. SA/CMS/urea was a glossy white particle when it was dried, and its transparency and size increased after water absorption. After covering the outer membrane of PDA, SA/CMS/PDA/urea appeared as black particles, and the transparency and particle size increased obviously after absorbing water. The SEM images showed that there were many granular protrusions on the surface of the SA/urea particles. The surface of SA/CMS/urea was relatively smooth and lustrous, with many tiny undulations and several folds. After covering it with PDA, the surface of SA/CMS/PDA/urea became smoother, but there were still some obvious large holes.

3.4. Water Absorption, Retention, and Water-Holding Capacity of SCPU

SCPU can improve the water-holding capacity of soil, thus storing water during irrigation or rainfall, and releasing water when facing water stress. The results showed that the water absorption of SA/urea was 19.1%. For SA/CMS/urea, it was increased to 164.9% with the addition of CMS. The water absorption of SA/CMS/PDA/urea was 169.5%, which may be attributed to the hydrophilicity of the PDA film (Figure 3A). It was reported that a kind of nitrogen slow-release fertilizer based on chitosan/polyvinyl alcohol blend also has a good water absorption of up to 120% [30]. For the soil without SCPU, the water holding capacity was 45.1% on the 10th day and decreased to 0.18% on the 16th day. For the soil with 5 g SCPU added, the water holding capacity was 77.2% on the 10th day, and it could still be maintained at 24.7% on the 20th day (Figure 3B). The water-holding ratio of untreated soil was 42.9%, while the ratios of soil treated with 3 g and 5 g SCPU were 72.0% and 80.4%, respectively. The results showed that the addition of SCPU was beneficial to reduce the speed of water loss and alleviate water stress (Figure 3C). It had been found that the water retention performance of soil with SRF was significantly higher than that of soil without SRF [36].

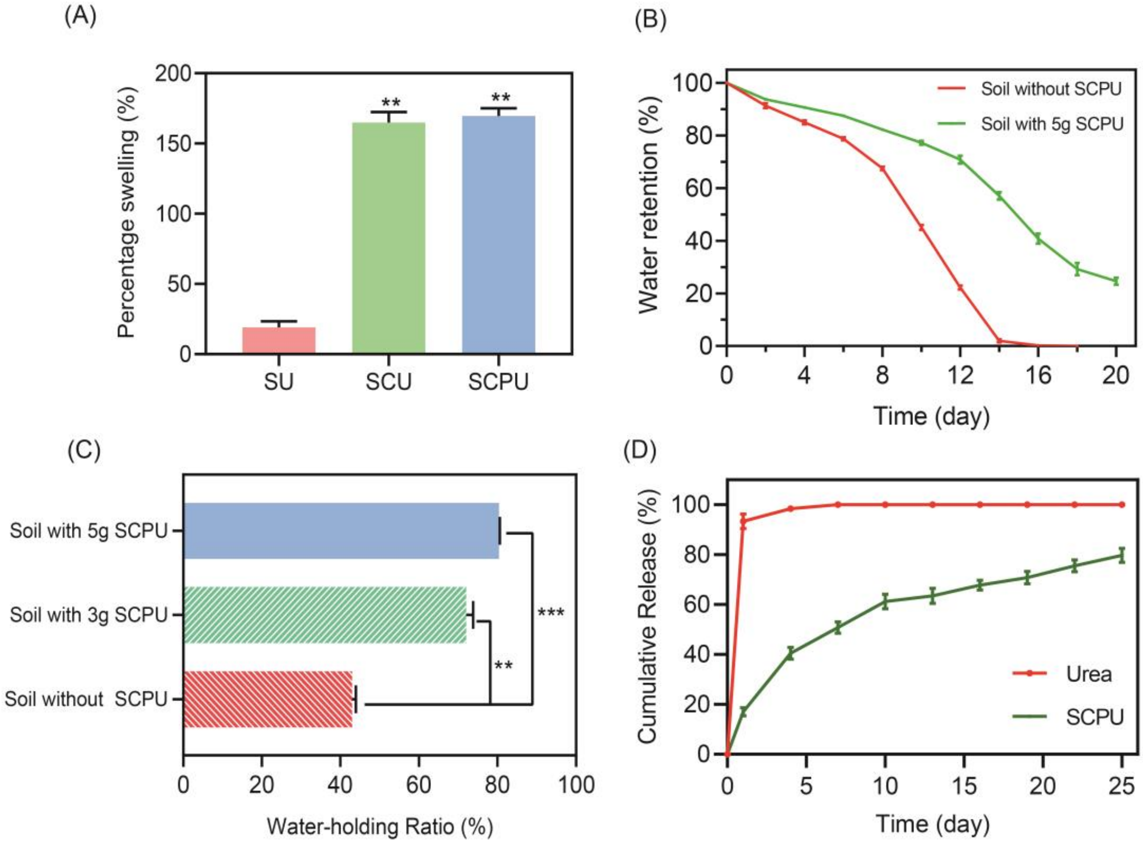

Figure 3. (**A**) Water absorption of SU, SCU, and SCPU. (**B**) Water retention, (**C**) water-holding ratio, and (**D**) cumulative release behavior in soil. ** $p < 0.01$, *** $p < 0.001$.

3.5. Slow-Release Behavior and Mechanism of SCPU in Soil

The release behavior and mechanism of SCPU in soil were studied at room temperature. In the soil treated with urea (CK), almost all urea was released on the 4th day. Compared with CK, the soil treated with SCPU released 79.7% of urea on the 25th day, indicating a longer duration (Figure 3D). For SCPU, the initial rapid release might be attributed to the release of urea loaded near the surface [37].

Four release kinetic models were used to simulate the behavior of SCPU in releasing urea. The release kinetic parameters of different models were shown in Table 1. The results showed that the Ritger–Peppas model (R^2 = 0.987) was the best-fitting model for urea release in soil. The diffusion constant in the Ritger–Peppas model can be used to determine diffusion mechanism of SCPU, which is similar to the release mechanism of a double-mesh hydrogel slow-release fertilizer based on sodium alginate and halloysite [33]. Since n = 0.392 ($\leq$0.45), the diffusion mechanism followed Fickian diffusion [38].

Table 1. Parameters of the kinetic model.

Model	Parameter	Value
Zero-order	R^2	0.814
	K_0	2.734
First-order	R^2	0.982
	K_1	0.168
Higuchi	R^2	0.973
	K_H	15.806
Ritger–Peppas	R^2	0.987
	n	0.392

3.6. Photothermal Conversion Effect

An appropriate amount of SCU and SCPU particles was placed in Petri dishes and irradiated in the sun for 5 min. During this process, the temperature change in particles was observed regularly with an infrared camera (Figure 4). The results showed that compared with SCPU, the temperature of SCPU particles, which were covered with PDA film, increased rapidly within 5 min. This indicated that SCPU fertilizer particles have a photothermal conversion ability, which was related to the photothermal conversion effect of the PDA film [39,40].

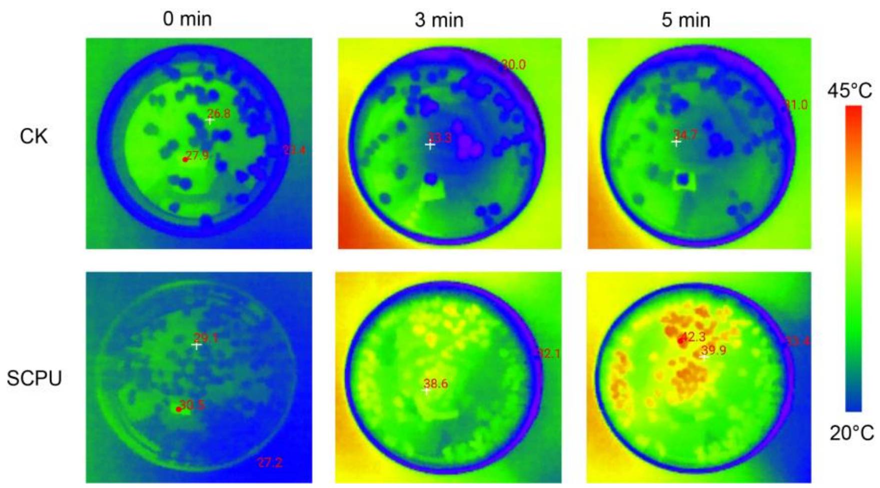

Figure 4. Infrared photos of SCU (CK) and SCPU under sunshine.

3.7. Effects of SCPU on the Growth of Winter Wheat

To evaluate the influence of SCPU on the growth of plants, winter wheat (Jimai 23) was selected as the model crop. In pot experiments, the performance levels of winter wheat in the untreated group (CK), urea group, 1× SCPU group (containing the same amount of urea), and 2× SCPU group (containing twice the amount of urea) were compared under normal growth conditions and water stress. The results of winter wheat growth are shown in Figure 5. The germination rate and height of winter wheat treated with SCPU were significantly higher than those of the CK and urea groups (Figure 5A,B). This may be related to the slow release of urea by SCPU and the growth promoting effect of PDA. In addition, in the process of water stress, winter wheat treated with SCPU can maintain growth for at least 9 days. However, the winter wheat of CK and urea groups had withered and died after drought for 9 days without watering (Figure 5C). This indicated that the application of SCPU could improve the drought resistance of winter wheat [41].

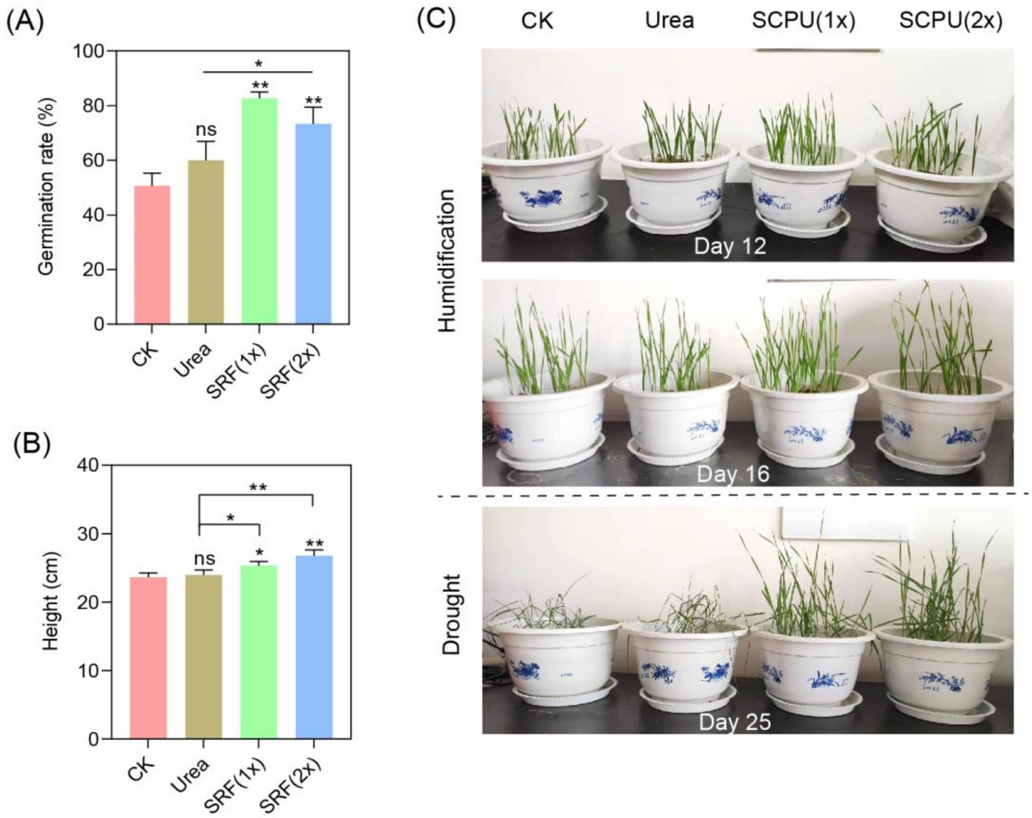

Figure 5. (**A**) Germination rate and (**B**) height of winter wheat treated with CK, urea, SCPU (1×), and SCPU (2×). (**C**) Growth of winter wheat in normal and drought environments. ns, not significant at the $p = 0.05$ level; * $p < 0.05$; ** $p < 0.01$.

The nitrogen nutrient released rapidly in urea far exceeds the utilization capacity of plants, which leads to higher losses. And the fast ammonia volatilization may affect the germination of plants [42,43]. On the contrary, the slow-release behavior of SCPU is milder, which can meet the requirements of plant growth. Previous studies have found that crop yields are influenced primarily by the amount and distribution of rainfall and the soil's capacity to hold moisture [44,45]. Thus, the improvement of soil water-holding capacity through treatment with SCPU is also one of the reasons for the better growth of winter wheat. Apart from these, the photothermal conversion effect of polydopamine is beneficial to the increase in soil temperature, and can play numerous physiological roles in plants, especially in improving plant nitrogen use efficiency [46]. These factors made the winter wheat grow better in the soil treated by SCPU.

Although SCUP is more beneficial to plant growth than pure urea, the application cost is also an important factor to be considered in the practical promotion of SCPU. After a cursory calculation and comparison (Table S1), the SCPU obtained relatively higher preparation price of 85 RMB·kg^{-1} compared with that of traditional urea fertilizer. Nevertheless, this price is lower than that of other similar products reported in the previous literature (226 RMB·kg^{-1}). Although the price of SCPU is not very competitive compared with traditional fertilizers, considering the yield and environmental benefits, this SRF may be a promising choice for proper optimization in some arid and cold areas in the future.

4. Conclusions

In conclusion, a slow-release urea fertilizer (SCPU) based on sodium alginate/carboxymethyl starch sodium/polydopamine was obtained by a two-step method. It was analyzed and characterized by FTIR, TGA, SEM, and infrared camera. Compared with sodium alginate particles, SCPU can significantly improve the water absorption. Further results showed that SCPU could increase the water holding capacity of soil, slow down the loss of water, and was sensitive to light. SCPU can release urea continuously in soil for more than 25 days, and the mechanism of release behavior was consistent with Fickian diffusion. The results of pot experiments showed that SCPU can promote the germination of winter wheat, improve growth, and enhance the drought resistance of crops. In summary, the findings of this study will help promote the growth of winter crops, prolong the duration of fertilizer, and improve soil moisture.

Supplementary Materials: The following supporting information can be downloaded at: https://www.mdpi.com/article/10.3390/pr12040842/s1, Table S1. Comparison of urea, SCPU, and other SRFs in practical application.

Author Contributions: Conceptualization, Y.L. and J.D.; methodology, Y.L.; validation, Y.M.; formal analysis, F.C., H.Z. and C.T.; writing—original draft preparation, Y.L.; writing—review and editing, J.D.; funding acquisition, Y.L., J.D. and C.T.; project administration, F.J. and Y.K. All authors have read and agreed to the published version of the manuscript.

Funding: This research was funded by the Science & Technology Program of Shaanxi Academy of Science (No. 2021k-16), the Science & Technology Program of Xi'an (No. 22NYYF034), the Key Research & Development Program of Shaanxi Province (No. 2023-YBNY-246), and the Key Technical Program in Agricultural Chains of Xi'an (No. 22NYGG0002).

Data Availability Statement: Data are contained within the article.

Acknowledgments: The graphical abstract was drawn by Figdraw.

Conflicts of Interest: Author C.T. was employed by Shaanxi Zhongkewanjia Agricultural Company. The authors declare that this study received funding from Shaanxi Zhongkewanjia Agricultural Company. The funder had the following involvement with the study: formal analysis. The remaining authors declare that the research was conducted in the absence of any commercial or financial relationships that could be construed as a potential conflict of interest.

References

1. Zheng, H.; Mei, P.; Wang, W.; Yin, Y.; Li, H.; Zheng, M.; Ou, X.; Cui, Z. Effects of super absorbent polymer on crop yield, water productivity and soil properties: A global meta-analysis. *Agric. Water Manag.* **2023**, *282*, 108290. [CrossRef]
2. Popova, Z.; Kercheva, M. CERES model application for increasing preparedness to climate variability in agricultural planning-risk analyses. *Phys. Chem. Earth.* **2005**, *30*, 117–124. [CrossRef]
3. Zhang, X.; Davidson, E.A.; Mauzerall, D.L.; Searchinger, T.D.; Dumas, P.; Shen, Y. Managing nitrogen for sustainable development. *Nature* **2015**, *528*, 51–59. [CrossRef] [PubMed]
4. Dimkpa, C.O.; Fugice, J.; Singh, U.; Lewis, T.D. Development of fertilizers for enhanced nitrogen use efficiency—Trends and perspectives. *Sci. Total Environ.* **2020**, *731*, 139113. [CrossRef] [PubMed]
5. Nooeaid, P.; Chuysinuan, P.; Pitakdantham, W.; Aryuwananon, D.; Techasakul, S.; Dechtrirat, D. Eco-Friendly polyvinyl alcohol/polylactic acid core/shell structured fibers as controlled-release fertilizers for sustainable agriculture. *J. Polym. Environ.* **2021**, *29*, 552–564. [CrossRef]
6. Yahaya, S.M.; Mahmud, A.A.; Abdullahi, M.; Haruna, A. Recent advances in the chemistry of nitrogen, phosphorus and potassium as fertilizer in soil: A review. *Pedosphere* **2023**, *33*, 385–406. [CrossRef]
7. Wen, P.; Han, Y.; Wu, Z.; He, Y.; Ye, B.C.; Wang, J. Rapid synthesis of a corncob-based semi-interpenetrating polymer network slow-release nitrogen fertilizer by microwave irradiation to control water and nutrient losses. *Arab. J. Chem.* **2017**, *10*, 922–934. [CrossRef]
8. Liu, L.; Zheng, X.; Wei, X.; Kai, Z.; Xu, Y. Excessive application of chemical fertilizer and organophosphorus pesticides induced total phosphorus loss from planting causing surface water eutrophication. *Sci. Rep.* **2021**, *11*, 23015. [CrossRef] [PubMed]
9. Azeem, B.; KuShaari, K.; Man, Z.B.; Basit, A.; Thanh, T.H. Review on materials & methods to produce controlled release coated urea fertilizer. *J. Control Release* **2014**, *181*, 11–21. [CrossRef]
10. Santos, A.C.S.; Henrique, H.M.; Cardoso, V.L.; Reis, M.H.M. Slow release fertilizer prepared with lignin and poly(vinylacetate) bioblend. *Int. J. Biol. Macromol.* **2021**, *185*, 543–550. [CrossRef]
11. Cong, J.; Lu, P.; Zhang, M. Preparation and Characterization of Environmentally Friendly Controlled Release Fertilizers Coated by Leftovers-Based Polymer. *Processes* **2020**, *8*, 417. [CrossRef]
12. Huang, J.; Chen, L.; Huang, M.; Liu, M. Urea intercalated halloysite/sodium alginate composite hydrogels for slow-release fertilizers. *Appl. Clay Sci.* **2023**, *242*, 107041. [CrossRef]
13. Alharbi, K.; Ghoneim, A.; Ebid, A.; El-Hamshary, H.; El-Newehy, M.H. Controlled release of phosphorous fertilizer bound to carboxymethyl starch-g-polyacrylamide and maintaining a hydration level for the plant. *Int. J. Biol. Macromol.* **2018**, *116*, 224–231. [CrossRef] [PubMed]

14. Lee, H.; Dellatore, S.M.; Miller, W.M.; Messersmith, P.B. Mussel-Inspired Surface Chemistry for Multifunctional Coatings. *Science* **2007**, *318*, 426–430. [CrossRef]
15. Xu, Y.; Zheng, D.; Chen, X.; Yao, W.; Wang, Y.; Zheng, Z.; Tan, H.; Zhang, Y. Mussel-inspired polydopamine-modified cellulose nanocrystal fillers for the preparation of reinforced and UV-shielding poly (lactic acid) films. *J. Mater. Res. Technol.* **2022**, *19*, 4350–4359. [CrossRef]
16. Du, P.; Yin, B.; Zhou, S.; Li, Z.; Zhang, X.; Cao, Y.; Han, R.; Shi, C.; Liang, B.; Xu, J. Melatonin and dopamine mediate the regulation of nitrogen uptake and metabolism at low ammonium levels in *Malus hupehensis*. *Plant Physiol. Bioch.* **2022**, *171*, 182–190. [CrossRef]
17. Suppanucroa, N.; Nimpaiboon, A.; Boonchuay, K.; Khamkeaw, A.; Phisalaphong, M. Green composite sponge of natural rubber reinforced with cellulose filler using alginate as a dispersing agent. *J. Mater. Res. Technol.* **2023**, *27*, 3119–3130. [CrossRef]
18. Aydınoğlu, D.; Karaca, N.; Ceylan, Ö. Natural Carrageenan/Psyllium Composite Hydrogels Embedded Montmorillonite and Investigation of Their Use in Agricultural Water Management. *J. Polym. Environ.* **2021**, *29*, 785–798. [CrossRef]
19. Olad, A.; Zebhi, H.; Salari, D.; Mirmohseni, A.; Tabar, A.R. Slow-release NPK fertilizer encapsulated by carboxymethyl cellulose-based nanocomposite with the function of water retention in soil. *Mat. Sci. Eng. C* **2018**, *90*, 333–340. [CrossRef]
20. Zheng, T.; Liang, Y.; Ye, S.; He, Z. Superabsorbent hydrogels as carriers for the controlled-release of urea: Experiments and a mathematical model describing the release rate. *Biosyst. Eng.* **2009**, *102*, 44–50. [CrossRef]
21. Bortolin, A.; Aouada, F.A.; Mattoso, L.H.C.; Ribeiro, C. Nanocomposite PAAm/methyl cellulose/montmorillonite hydrogel: Evidence of synergistic effects for the slow release of fertilizers. *J. Agric. Food Chem.* **2013**, *61*, 7431–7439. [CrossRef]
22. Olad, A.; Gharekhani, H.; Mirmohseni, A.; Bybordi, A. Study on the synergistic effect of clinoptilolite on the swelling kinetic and slow release behavior of maize bran-based superabsorbent nanocomposite. *J. Polym. Res.* **2016**, *23*, 241. [CrossRef]
23. Li, Q.; Ma, Z.; Yue, Q.; Gao, B.; Li, W.; Xu, X. Synthesis, characterization and swelling behavior of superabsorbent wheat straw graft copolymers. *Bioresour. Technol.* **2012**, *118*, 204–209. [CrossRef] [PubMed]
24. Fernandes, R.S.; Moura, M.R.; Glenn, G.M.; Aouada, F.A. Thermal, microstructural, and spectroscopic analysis of Ca^{2+} alginate/clay nanocomposite hydrogel beads. *J. Mol. Liq.* **2018**, *265*, 327–336. [CrossRef]
25. Dankar, I.; Haddarah, A.; Omar, F.E.L.; Pujola, M.; Sepulcre, F. Characterization of food additive-potato starch complexes by FTIR and X-ray diffraction. *Food Chem.* **2018**, *260*, 7–12. [CrossRef] [PubMed]
26. Kaczmarska, K.; Grabowska, B.; Spychaj, T.; Zdanowicz, M.; Sitarz, M.; Bobrowski, A.; Cukrowicz, S. Effect of microwave treatment on structure of binders based on sodium carboxymethyl starch: FT-IR, FT-Raman and XRD investigations. *Spectrochim. Acta A* **2018**, *199*, 387–393. [CrossRef] [PubMed]
27. Li, Y.; Su, Y.; Zhao, X.; He, X.; Zhang, R.; Zhao, J.; Fan, X.; Jiang, Z. Antifouling, High-flux Nanofiltration Membranes Enabled by Dual Functional Polydopamine. *ACS Appl. Mater. Interfaces* **2014**, *6*, 5548–5557. [CrossRef]
28. Yadav, T.; Mukherjee, V. Interpretation of IR and Raman spectra of dopamine neurotransmitter and effect of hydrogen bond in HCl. *J. Mol. Struct.* **2018**, *1160*, 256–270. [CrossRef]
29. Zangmeister, R.A.; Morris, T.A.; Tarlov, M.J. Characterization of polydopamine thin films deposited at short times by autoxidation of dopamine. *Langmuir* **2013**, *29*, 8619–8628. [CrossRef] [PubMed]
30. Vo, P.T.; Nguyen, H.T.; Trinh, H.T.; Nguyen, V.M.; Le, A.T.; Tran, H.Q.; Nguyen, T.T.T. The nitrogen slow-release fertilizer based on urea incorporating chitosan and poly (vinyl alcohol) blend. *Environ. Technol. Innov.* **2021**, *22*, 101528. [CrossRef]
31. Cai, X.; Du, X.; Cui, D.; Wang, X.; Yang, Z.; Zhu, G. Improvement of stability of blueberry anthocyanins by carboxymethyl starch/xanthan gum combinations microencapsulation. *Food Hydrocoll.* **2019**, *91*, 238–245. [CrossRef]
32. Elhassani, C.E.; Essamlali, Y.; Aqlil, M.; Nzenguet, A.M.; Ganetri, I.; Zahouily, M. Urea-impregnated HAP encapsulated by lignocellulosic biomass-extruded composites: A novel slow-release fertilizer. *Environ. Technol. Innov.* **2019**, *15*, 100403. [CrossRef]
33. Shen, Y.; Wang, H.; Li, W.; Liu, Z.; Liu, Y.; Wei, H.; Li, J. Synthesis and characterization of double-network hydrogels based on sodium alginate and halloysite for slow release fertilizers. *Int. J. Biol. Macromol.* **2020**, *164*, 557–565. [CrossRef]
34. Zhang, B.; Sun, B.; Li, X.; Yu, Y.; Tian, Y.; Xu, X.; Jin, Z. Synthesis of pH- and ionic strength-responsive microgels and their interactions with lysozyme. *Int. J. Biol. Macromol.* **2015**, *79*, 392–397. [CrossRef]
35. Shanmuganathan, K.; Cho, J.H.; Iyer, P.; Baranowitz, S.; Ellison, C.J. Thermooxidative stabilization of polymers using natural and synthetic melanins. *Macromolecules* **2011**, *44*, 9499–9507. [CrossRef]
36. Wei, H.; Wang, H.; Chu, H.; Li, J. Preparation and characterization of slow-release and water retention fertilizer based on starch and halloysite. *Int. J. Biol. Macromol.* **2019**, *133*, 1210–1218. [CrossRef] [PubMed]
37. Kenawy, E.R.; Azaam, M.M.; El-nshar, E.M. Sodium alginate-g-poly(acrylic acid-co-2-hydroxyethyl methacrylate)/montmorillonite superabsorbent composite: Preparation, swelling investigation and its application as a slow-release fertilizer. *Arab. J. Chem.* **2019**, *12*, 847–856. [CrossRef]
38. Ebadi, A.; Rafati, A.A.; Bavafa, S.; Mohammadi, M. Kinetic and theoretical studies of novel biodegradable thermo-sensitive xerogels based on PEG/PVP/silica for sustained release of enrofloxacin. *Appl. Surf. Sci.* **2017**, *425*, 282–290. [CrossRef]
39. Babavalian, A.; Tekie, F.S.M.; Ayazi, H.; Ranjbar, S.; Varshochian, R.; Rad-Malelkshahi, M.; Akhavan, O.; Dinarvand, R. Reduced polydopamine coated graphene for delivery of Hset1 antisense as a photothermal and gene therapy of breast cancer. *J. Drug Deliv. Sci. Technol.* **2022**, *73*, 103462. [CrossRef]

40. Wang, D.; Wu, H.; Zhou, J.; Xu, P.; Wang, C.; Shi, R.; Wang, H.; Wang, H.; Guo, Z.; Chen, Q. In situ one-pot synthesis of MOF-Polydopamine hybrid nanogels with enhanced photothermal effect for targeted cancer therapy. *Adv. Sci.* **2018**, *5*, 1800287. [CrossRef]
41. Dong, G.; Mu, Z.; Liu, D.; Shang, L.; Zhang, W.; Gao, Y.; Zhao, M.; Zhang, X.; Chen, S.; Wei, M. Starch phosphate carbamate hydrogel based slow-release urea formulation with good water retentivity. *Int. J. Biol. Macromol.* **2021**, *190*, 189–197. [CrossRef] [PubMed]
42. Rahman, M.H.; Haque, K.M.S.; Khan, M.Z.H. A review on application of controlled released fertilizers influencing the sustainable agricultural production: A Cleaner production process. *Environ. Technol. Innov.* **2021**, *23*, 101697. [CrossRef]
43. Wan, X.; Wu, W.; Li, C.; Liu, Y.; Wen, X.; Liao, Y. Soil ammonia volatilization following urea application suppresses root hair formation and reduces seed germination in six wheat varieties. *Environ. Exp. Bot.* **2016**, *132*, 130–139. [CrossRef]
44. Lawes, R.A.; Oliver, Y.M.; Robertson, M.J. Integrating the effects of climate and plant available soil water holding capacity on wheat yield. *Field Crop. Res.* **2019**, *113*, 297–305. [CrossRef]
45. Paradelo, R.; Basanta, R.; Barral, M.T. Water-holding capacity and plant growth in compost-based substrates modified with polyacrylamide, guar gum or bentonite. *Sci. Hortic.-Amst.* **2019**, *243*, 344–349. [CrossRef]
46. Du, P.; Yin, B.; Cao, Y.; Han, R.; Ji, J.; He, X.; Liang, B.; Xu, J. Beneficial effects of exogenous melatonin and dopamine on low nitrate stress in *Malus hupehensis*. *Front. Plant Sci.* **2022**, *28*, 807472. [CrossRef]